

be a consequence of these carbons being positioned near to the paramagnetic heme iron ion, as previously discussed.<sup>13</sup> It implies, again, that the primary interaction between chloroquine and urohemim I is also a  $\pi$ - $\pi$  type complex between aromatic moieties. Furthermore, considering the 2:1 stoichiometry (heme-drug) revealed by Job's method, a sandwich-type complex (Figure 7A) is consistent with all of our data. This structure resembles the structure for the quinine-urohemim I complex, which has identical stoichiometry.<sup>13</sup>

Urohemim I association with quinine and chloroquine results in solution complexes of identical stoichiometry. The quinine association is cooperative (Hill parameter = 2),<sup>13</sup> while the chloroquine association is noncooperative (Hill parameter = 1). For quinine, the source of cooperativity, consistent with the other spectroscopic data, was postulated to be the 9-OH group coordination to the heme iron, in addition to the  $\pi$ - $\pi$  association. This accounted for two inequivalent binding sites on urohemim I. The data presented here add further support to this view, which was first identified by Behere and Goff,<sup>30</sup> by revealing that chloroquine, a structurally related drug that has no donor group capable of coordinating to heme iron simultaneous with  $\pi$ - $\pi$  association, does not exhibit cooperativity.

Finally, a comparison of the overall apparent equilibrium constants determined under identical conditions for chloroquine

(Table I) and quinine<sup>13</sup> is warranted. If hemes are truly the drug receptors, the data of Table I suggest that differences in the efficacy of the two drugs is not attributable to different binding constants. For a common heme (urohemim I),  $K_A(\text{app})$  has the same order of magnitude for both drugs. Such is not the case for binding to uroporphyrin I where chloroquine exhibits an affinity approximately 2 orders of magnitude higher than quinine does. We attribute this to the more complete  $\pi$ - $\pi$  type interaction that is possible for chloroquine in our model of the complex (Figure 7B) rather than the peripheral complex model, with less  $\pi$ - $\pi$  overlap, found for quinine.

**Acknowledgment.** We gratefully acknowledge support for this work from the National Institutes of Health (Grants 2R01DK30912 and K04HL10175) and the Alfred P. Sloan Foundation. NMR spectra were obtained on an instrument whose purchase was made possible by a grant from the National Science Foundation (Grant CHE 820134). We also wish to acknowledge stimulating discussions with Dr. John Shelnett, Sandia National Laboratories, and the use of his nonlinear least squares fitting program for coupled equations.

**Registry No.** Chloroquine, 54-05-7; urohemim I chloride, 92284-96-3; uroporphyrin I, 607-14-7; urohemim I-chloroquine complex, 114422-76-3; uroporphyrin I-chloroquine complex, 114422-77-4.

## Monolayer Properties of Eight Diastereomeric Two-Chain Surfactants at the Air/Water Interface: A Resultant of Intramolecular and Intermolecular Forces

Noel Harvey, Philip Rose, Ned A. Porter, Jeffrey B. Huff, and Edward M. Arnett\*

Contribution from the Department of Chemistry, Duke University, Durham, North Carolina 27706. Received November 3, 1987

**Abstract:** Force-area isotherms, equilibrium spreading pressures, free energies of activation to viscous flow, and surface viscosities are reported for four pairs of diastereomeric surfactants made by joining two pentadecanoic acid units by a carbonyl group at the 3,3', 6,6', 9,9', and 12,12'-positions. The eight compounds are four pairs of diastereomers (meso, *dl*) that differ only by the position of the carbonyl cross-link. Accordingly, any differences in their surface properties must have a stereochemical origin. In all cases the meso monolayers are compressed more easily than their *dl* diastereomers. This is attributed to the more facile aggregation (easier packing) of the former as a result of their lowest energy conformations, which give good lateral alignment of the hydrocarbon chains about the meso plane of symmetry when both carboxylate groups are in the water surface. In contrast, the *dl* compounds are forced into a higher energy conformation if the chains are brought into alignment while the carboxylate groups are in the surface, since the lowest energy *dl* conformation is one in which the head groups are separated by the largest possible longitudinal distance in the surface of the water. This results in resistance of the *dl* films to compression and reduces the attraction between their chains as compared to meso films. This is to our knowledge the first systematic study of the monolayer properties of a diastereomeric series.

A decade ago we initiated an investigation of the effects of introducing chiral centers into surfactants on their intermolecular forces as reflected by their properties as monolayers at the air/water interface. There were virtually no published accounts on the topic available at that time. All of the work we have done in the interim shows clearly that, with the notable exception of the phosphatidylcholines,<sup>1</sup> essentially all of the surface properties of all of the surfactants we have studied to date are strongly stereoselective in that they show chiral discrimination between the properties of pure enantiomers and their racemic mixtures.

In the course of another project, reported elsewhere,<sup>2</sup> four pairs of diastereomeric diacids consisting of two *n*-pentadecanoic acids bonded together at the 3-, 6-, 9-, and 12-carbons by a carbonyl group were synthesized. When they were epimerized in aqueous base at 60 °C, at concentrations above the critical micelle concentration (CMC), all of them showed a preference for the meso form in accordance with predictions from molecular mechanics. However, epimerization in homogeneous media (e.g., benzene solution, TsOH catalyst) or in water (<sup>-</sup>OH catalyst) below the CMC gave 50:50 mixtures of meso and *dl* diastereomers. It was thus concluded that hydrophobic forces perturb the equilibrium

(1) (a) Arnett, E. M.; Gold, J. M. *J. Am. Chem. Soc.* 1982, 104, 636. (b) Arnett, E. M.; Gold, J. M.; Harvey, N. G.; Whitesell, L. G. In *New Applications of Phospholipid Bilayers, Thin Films and Vesicles*; Plenum: New York, in press.

(2) (a) Porter, N. A.; Ok, D.; Adams, C. M.; Huff, J. B. *J. Am. Chem. Soc.* 1986, 108, 5025. (b) Porter, N. A.; Ok, D.; Huff, J. B.; Adams, C. M.; McPhail, A. T.; Kim, K. *J. Am. Chem. Soc.* 1988, 110, 1896.

between diastereomers in favor of the meso form. The present article reports a study of these eight diastereomeric compounds as monolayers at the air/water interface—a special set of circumstances representing an extreme of hydrophobic control in which intermolecular and intramolecular forces may be opposed directly. This article is the first comparison, to our knowledge, of a set of diastereomeric monolayers, and it also describes a unique application of a Verger film balance<sup>3</sup> for the determination of surface viscosity by allowing isobaric monolayer flow through a slit of carefully controlled dimensions.

### Experimental Section

In view of the extreme sensitivity of monolayers to contamination and the resulting likelihood of erroneous results, every precaution was taken to ensure that all materials and instruments used in this study were clean. Steps toward this end have been described elsewhere.<sup>4</sup>

**Materials Preparation and Purification.** The four two-chain diastereomeric dicarboxylic acid pairs were prepared and separated as described previously.<sup>2</sup> Purification was achieved by reverse-phase HPLC (Dynamax Macro columns, Rainin Corp.). The eluting solvent was CH<sub>3</sub>CN/H<sub>2</sub>O/AcOH, having ratios of 99:1:0.1 (C-3,3'), 85:15:0.1 (C-6,6', C-9,9'), and 90:10:0.1 (C-12,12'). Acceptable spectral data and carbon and hydrogen combustion analyses within  $\pm 0.4$  C and  $\pm 0.4$  H were obtained for all compounds. The surfactants were stored in clean glassware after their purification.

**Spreading Solutions.** Each diastereomer was weighed for solution preparation on a Cahn RG electrobalance as described previously.<sup>4</sup> The typical spreading solution was made by dissolving 3–4 mg of surfactant into 25 mL of highly purified 9:1 hexanes/EtOH in hand-calibrated 25-mL volumetric flasks. This gave solutions with accurately determined concentrations of  $2.349 \times 10^{-4}$ – $3.130 \times 10^{-4}$  M.

The surfactant was delivered dropwise to the air/water interface, with a separate Agla microliter syringe (Burrhoughs-Wellcome, No. MS-01) for each diastereomer. Special care was taken to ensure that spreading solutions and syringes were kept in thermal equilibrium. Spreading solutions were stored under an atmosphere of hexanes in a clean desiccator at a constant  $25.0 \pm 0.1$  °C.

The proper amount of each diastereomer to be delivered to the surface was determined in "scouting" runs performed by delivering  $4.403 \times 10^{16}$  molecules to a typical area of  $6.84 \times 10^{18}$  Å<sup>2</sup>. Solutions that formed highly expanded films at greater than 100 Å<sup>2</sup>/molecule were spread by using smaller aliquots of spreading solution until the entire isotherm from  $\Pi \approx 0$  to approximately 40 dyn/cm could be recorded.

**Subphase Water.** The subphase water used in all experiments was triply distilled and purified as described previously.<sup>4</sup>

**Langmuir Film Balance Techniques.** The cleaning, preparation, calibration, and technical specifications of the Langmuir film balance have been described in detail.<sup>4</sup> The balance has been further outfitted with an analog to digital converter system (constructed by Dr. Eric Johnson) interfaced with an Apple II computer so that data may be recorded and stored on a floppy disk as well as on the strip-chart recorder.

The rate of compression for each monolayer film was varied from 7.1 to 29.8 Å<sup>2</sup>/molecule per min. No difference was seen in the  $\Pi/A$  isotherms within this compression range. For all reported isotherms the rate of compression was kept constant at 19.2 Å<sup>2</sup>/molecule per min.

Each film of every *dl* and meso diastereomer and their mixtures was compressed to as high a surface pressure as possible without breaking the positive meniscus of the balance ( $\approx 40$  dyn/cm) and immediately reexpanded at the same rate. Each diastereomer and mixed diastereomer isotherm was obtained at  $23.8 \pm 0.3$  °C and reproduced 5–12 times. The stability of the films was checked once every six replications by compressing to a fixed surface pressure and halting compression for a minimum of 3 min. The validity of the film balance calibration was checked every 12 h with the well-known stearic acid isotherm.<sup>5</sup>

**Surface Viscometer.** Surface viscosity data were taken on a Verger "zero-order" film balance<sup>3</sup> modified for surface shear viscosity measurements. Since this type of system has not been used previously for precise measurement of surface viscosities, we will describe it in some detail here.

Figure 1 shows the rectangular trough as constructed of milled Teflon mounted on an aluminum base to prevent warping. The base is set on three legs with adjustable leveling screws attached to a movable aluminum plate. The entire setup is enclosed in a temperature-controlled

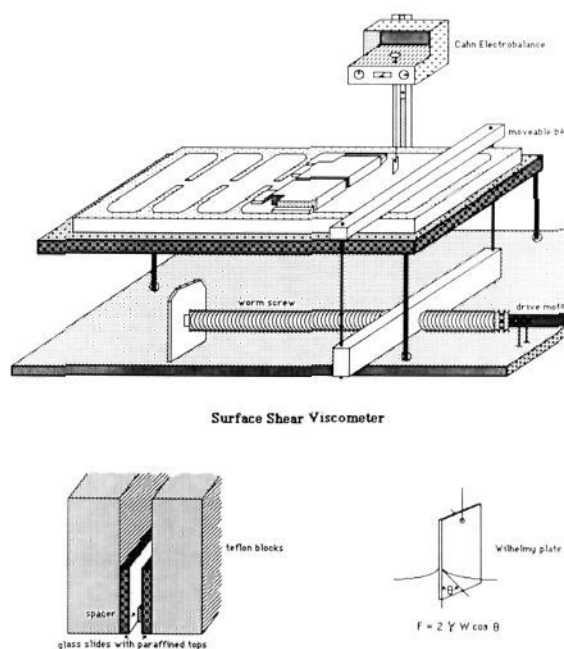


**Figure 1.** Detail of the Verger film balance modified for measurement of surface shear viscosity.

cabinet thermostated to  $\pm 0.5$  °C. The trough is divided into four compartments: one main trough ( $270 \times 175 \times 5$  mm) and three smaller troughs ( $74 \times 175 \times 5$  mm). Each compartment is connected by a small canal ( $10 \times 4 \times 1$  mm). The isthmus is designed to provide for diffusive film flow between compartments rather than viscous flow, thus avoiding a limiting step due to the surface viscosity of the film during the transfer from one compartment to the other.

The surface tension is measured by a  $22 \times 10$  mm paper Wilhelmy plate (Whatman filter paper) connected by a thin wire hook to a Cahn, Model RHL, electrobalance. The electrobalance is sensitive to  $\pm 0.1$  dyn/cm. The electrobalance output voltage is coupled through a feedback mechanism to a movable barrier. Any deviation from a preset value of surface tension will be compensated automatically by a movement of the barrier. This allows for the maintenance of a preset and constant surface pressure for a monomolecular film at the air/water interface. The movable barrier is constructed of Teflon and driven by a worm-screw assembly that is mounted beneath the trough. The reversible motor (Globe Industry, No. 319A128-21) and feedback controller maintain constant speeds from 0 to 48.5 mm/min.

The canal used in this viscometer was constructed of two glass slides 7.62 cm long, 1 mm wide, and 7 mm high. The depth of the canal was limited by the depth of the trough. The top edges of the glass slides were paraffined to render them hydrophobic, ensuring that the canal width did not vary due to formation of a meniscus. The slides were positioned in the subphase so the top edge of the canal was just even with water level. The canal width was held constant by small Plexiglas spacers (milled to  $1.5 \pm 0.1$  mm) resting on the bottom of the Teflon trough between the glass slides. The canal and spacer were sandwiched between two Teflon blocks holding the canal assembly in the center of the trough. Additional Teflon spacers were placed on either side of the large Teflon blocks isolating the subphase in the large trough from the smaller troughs except by way of the canal. The slit width can be varied by placing Plexiglas spacers of varying width between the glass slides and adjusting the Teflon spacers to either side of the large Teflon blocks.

Surface viscosity measurements were performed by first setting the electrobalance output voltage to zero for an air/water interface containing no surfactant. Milligram weights corresponding to the desired surface pressure in terms of the downward force,  $F$ , on the Wilhelmy plate ( $F = 2W\gamma \cos \theta$ ;  $\theta$  = contact angle) were placed on the electrobalance pan. Stock solution of surfactant was added dropwise to the surface of the large trough by a pipet fitted with a rubber bulb until a surface pressure was noted by a drop in balance output voltage. After allowing for evaporation of spreading solvent, a minimum of 15 min, the monolayer was compressed to the desired surface pressure. The system was allowed to equilibrate for an additional 15 min. The canal was then "opened" by bridging the isthmus between the large trough and the smaller troughs with subphase and the monolayer allowed to flow for 5 min. The position of the barrier was monitored by strip-chart recorder. The rate of viscous flow could then be calculated ( $\text{cm}^2/\text{s}$ ) from the slope

(3) Verger, R.; de Haas, G. H. *Chem. Phys. Lipids* 1973, 10, 127.

(4) Arnett, E. M.; Chao, J.; Kinzig, B.; Stewart, M.; Thompson, O.; Verbiar, R. *J. Am. Chem. Soc.* 1982, 104, 389.

(5) Gaines, G. L. *Insoluble Monolayers at Liquid-Gas Interfaces*; Wiley: New York, 1966, p 220.

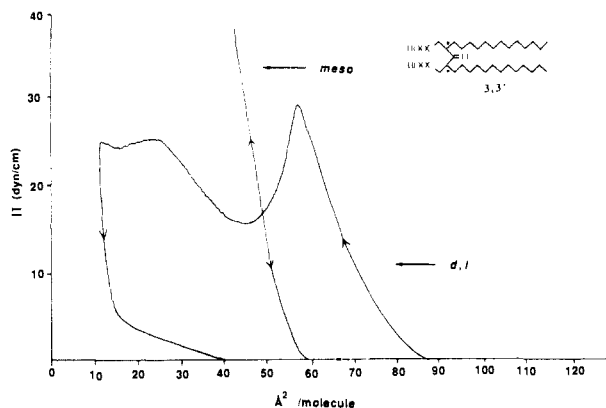


**Figure 2.** Surface pressure–area isotherms for the compression–expansion cycle of *dl* and *meso* 3,3'-diacid surfactants on a pure water subphase at 25 °C compressed at a rate of 19.24 Å<sup>2</sup>/molecule per min.

of the line recorded on the strip-chart and the surface viscosity calculated from the relation shown in eq 1, where  $\Pi_2 - \Pi_1$  is the difference in

$$\eta = (\Pi_2 - \Pi_1)\omega^3 / 12QL \quad (1)$$

surface pressure between the film-covered surface and pure water,  $\omega$  is the canal width,  $L$  is the canal length, and  $Q$  is the rate of film flow.<sup>6</sup> (Because we are only interested in the comparison of surface viscosities for *dl* and *meso* diastereomers, the classical correction for vicinal drag of the water subphase ( $\omega\eta_0/\Pi$ ) was not included in the viscosity calculations.) All surface viscosities were repeated a minimum of five times at each surface pressure. The surface was swept clean by aspiration with a clean pipet fitted to a vacuum filtration flask after each run, and a new monolayer was deposited.

The free energy of activation for viscous flow was calculated from the Moore–Eyring equation<sup>7</sup> (2), where  $\eta$  is the surface shear viscosity,  $h$  is Plank's constant, and  $a$  is the area per molecule obtained from the pressure vs area isotherms.

$$\eta = (h/a)e^{\Delta G^\ddagger / \kappa T} \quad (2)$$

As a check of the accuracy of this setup, the surface shear viscosities of *n*-tetradecanol ( $0.29 \pm 0.06$  surface mP), *n*-hexadecanol ( $1.12 \pm 0.10$  surface mP), and *n*-octadecanol ( $1.70 \pm 0.20$  surface mP) on a 0.01 N H<sub>2</sub>SO<sub>4</sub> subphase at 3.0 dyn/cm and those of hexadecanoic ( $0.93 \pm 0.16$  surface mP) and octadecanoic acid ( $0.93 \pm 0.08$  surface mP) on pure water at 2.5 dyn/cm were reproduced to good agreement with the values reported by Jarvis<sup>8</sup> and Joly.<sup>9</sup>

**Equilibrium Spreading Pressures (ESPs).** ESPs of each surfactant on pure water at 24.0 °C were determined by Du Nuoy ring tensiometry<sup>4</sup> on either a Fisher Autotensiometer or a manual Cenco Du Nuoy tensiometer (No. 70535). Before each measurement, the ring was cleaned by flaming and the surface tension of the freshly aspirated water surface taken. In each experiment, 0.5–1.0 mg of surfactant crystal, far in excess of the amount needed to form a monolayer, was carefully delivered to the subphase surface of a 6.8-cm-diameter Teflon dish (Autotensiometer) or a 6.5-cm-diameter T-cup (Cenco). The crystals were allowed to equilibrate a minimum of 18 h, with successive experiments being performed at 24 and 36 h. Equilibration was assumed when the readings changed by no more than 0.2 dyn/cm in a 4-h period. Each experiment was repeated with fresh subphase and crystals at least three times.

**Data Analysis.** All data reported here are analyzed at the 95% confidence limit by using "Student's *t*" for 5–12 repetitions for  $\Pi/A$  isotherms and surface viscosities and 3–6 repetitions for ESPs. The relatively large errors reported for  $\Delta\Delta G^\ddagger$  flow are a result of error propagation for surface shear viscosity, area per molecule, and each  $\Delta G^\ddagger$  flow calculation.

## Results and Discussion

**$\Pi/A$  Isotherms.** Figures 2–5 compare the position of the bridging carbonyl group in each diastereomeric pair and the effects of stereochemistry on their force–area curves at 25 °C. Several facts are striking. (a) In every case there is a sharp differentiation

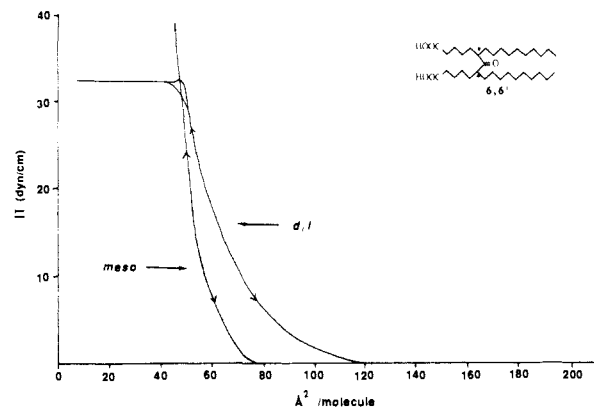


**Figure 3.** Surface pressure–area isotherms for the compression–expansion cycle of *dl* and *meso* 6,6'-diacid surfactants on a pure water subphase at 25 °C compressed at a rate of 19.24 Å<sup>2</sup>/molecule per min.

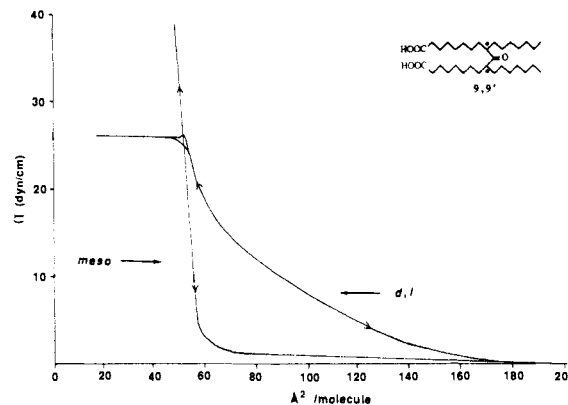


**Figure 4.** Surface pressure–area isotherms for the compression–expansion cycle of *dl* and *meso* 9,9'-diacid surfactants on a pure water subphase at 25 °C compressed at a rate of 19.24 Å<sup>2</sup>/molecule per min.

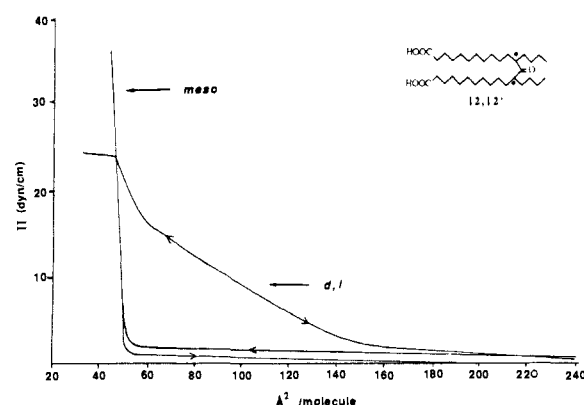


**Figure 5.** Surface pressure–area isotherms for the compression–expansion cycle of *dl* and *meso* 12,12'-diacid surfactants on a pure water subphase at 25 °C compressed at a rate of 19.24 Å<sup>2</sup>/molecule per min.

between the behavior of the *meso* and *dl* isomers. (b) The isotherms for the *meso* isomers are virtually identical at surface pressures greater than 5 dyn/cm regardless of the position of the carbonyl bridge, whereas the curves for the *dl* isomers are strongly dependent on the position of the bridge. (c) The limiting molecular area for the *meso* compounds is in the neighborhood of 60 Å<sup>2</sup> per molecule, and their isotherms are highly reminiscent of those for the single-chain fatty acids in the condensed phase. In contrast, the *dl* acids show more highly expanded films at lower pressures and have collapse pressures that are highly dependent on the position of the carbonyl connection.

These results are quite compatible with previous considerations of the preferred conformations of the two-chain carbonyl diacids in aqueous media.<sup>2</sup> As stated before, the *meso* compounds are more stable in molecular aggregates by about 1.2 kcal/mol than

(6) Harkins, W. D.; Kirkwood, J. G. *Nature (London)* **1948**, *141*, 38.

(7) Eyring, H.; Moore, W. J. *J. Chem. Phys.* **1938**, *6*, 391.

(8) Jarvis, N. L. *J. Phys. Chem.* **1965**, *69*(6), 1789.

(9) Joly, M. *J. Colloid Interface Sci.* **1956**, *11*, 519.

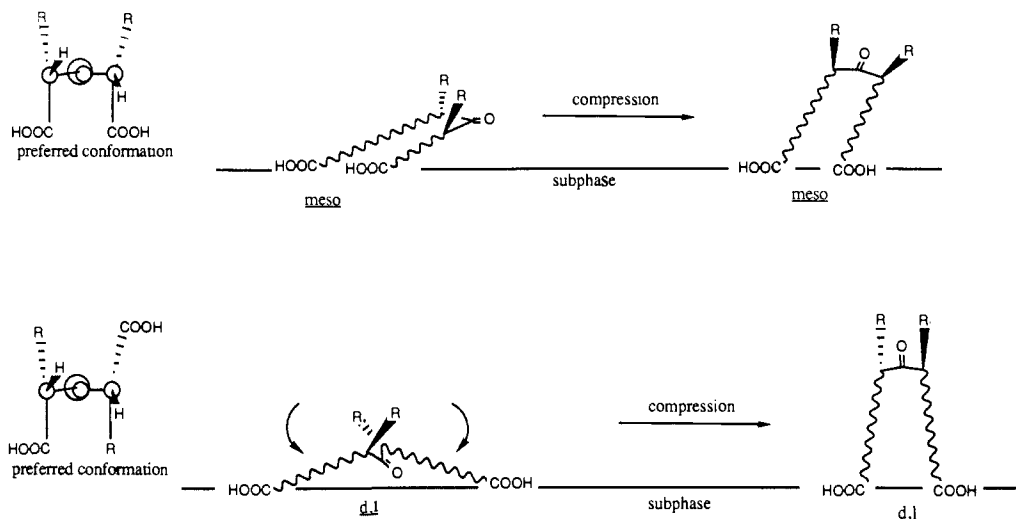


**Figure 6.** Preferred lowest energy conformations of *dl* and *meso* diastereomers and the effect of configurational stereochemistry on the mechanism of film compression.

**Table I.**

compd	equiv spreading pressure, dyn/cm	
	<i>meso</i>	<i>dl</i>
3,3'	15.48 ± 0.84	0.97 ± 1.36
6,6'	17.90 ± 0.84	12.93 ± 0.76
9,9'	16.75 ± 1.43	20.73 ± 3.82
12,12'	3.45 ± 0.43	10.45 ± 0.56

their *dl* isomers because of a preferred collinear conformation of the two chains that places the hydrogens at the asymmetric carbons in a nearly eclipsed position relative to each other (Figure 6). In this conformation, the two carboxylic acid groups at the ends of the chain can be attached to the water surface side-by-side and the entire molecule behaves as a "good amphiphile" whose structure is similar to a pair of single-chain fatty acid molecules bound side-by-side, each chain "mirroring" the other about the molecule's plane of symmetry.

In contrast, the *dl* isomers are most stable if the carboxylic acid groups are separated, with a rather wide range of pseudotorsional angles through which the groups around the bridging carbonyl can be twisted until a maximum energy is reached when they are nearly eclipsed. When one of the *dl* diacids is spread on an aqueous surface, the carboxylic acid groups are separated from each other and the entire molecule is spread out like a pair of open shears or hedge clippers on the surface (Figure 6). Since the fatty acid chains are separated longitudinally from each other, the molecule takes up more space on the surface and produces a more expanded monolayer, typical of "bolaform" amphiphiles.<sup>10-13</sup> The steady progression in expansion at low surface pressures is correlated with the position of a carbonyl bridge at carbons 3, 6, 9, and 12.

As the surface area is reduced and the carboxylate groups are forced together (equivalent to closing the shears), the chains are gradually brought into a position of collinearity and forced out of the surface to a standing position similar to that proposed for the *meso* diacid under similar compression. However, for the *dl* acids, in addition to the work of detaching the hydrocarbon chains from the surface, more work has to be done against intramolecular conformational forces to bring the chains together. The further apart the carboxylate groups are to begin with the greater is this  $\Pi/A$  work and the greater the integrated area under the curve.

**Equilibrium Spreading Pressures.** Table I shows the equilibrium spreading pressures (ESPs) of each diacid. It is immediately

apparent that for three of the diastereomeric pairs there are significant differences in the spontaneous spreading of *dl* vs *meso* monolayers in equilibrium with their respective bulk solid phases. However, there appears to be no discernable trend in either the *dl* or *meso* ESPs as a function of carbonyl position.

**Film Stability.** The stability of each diastereomer was checked by compressing a film (spread from hexanes/ETOH solution) to a given surface pressure and halting compression. In general, both the *dl* and *meso* compounds of each diastereomeric set decayed no more than 0.1 dyn/cm in the 3–5 min immediately following the halt of compression at surface pressures below the ESP. The exception to this rule was the *meso* 12,12'-compound, which showed immediate surface pressure decay (>1 dyn/cm per min) at any  $\Pi > 0$ .

Definite differences in film stability above the ESP were noted for each *dl*/*meso* pair. In all cases, the *meso* spread films were unstable ( $\Pi$  decaying at >1.0 dyn/cm per min) above the ESP, while the *dl* films appeared to be metastable ( $\Pi$  decaying at <0.2 dyn/cm per min) at pressures above their ESPs.

These phenomena indicate that the *meso* monolayers undergo either a slow collapse to a bulk phase or a significant relaxation due to reorganization or dissolution at surface pressures above their ESPs. The *dl* films appear to undergo this collapse or relaxation at a much slower rate, if at all.

**Phase Transitions.** It is readily apparent that the *dl* 6,6', 9,9', and 12,12'-compounds show a collapse to some 3-dimensional state, as has been observed for most overcompressed lipid films.<sup>14,15</sup> The surprising result is that the ensuing plateau region is extraordinarily stable, decaying in surface pressure no more than 0.1 dyn/cm per h when compression is halted. In accordance with the "2-dimensional" phase rule of Defay and Crisp,<sup>16,17</sup> this indicates that there are two phases in equilibrium, most likely consisting of monolayer and 3-dimensional aggregates. In addition, overcompression in this plateau region does not result in increased surface pressure even if the moving barrier of the film balance is run up to the detection barrier of the torsion head. The exact nature of the "collapsed" phases in this plateau region is not clear.

#### Surface Viscosity

In view of the dramatic diastereomeric effects on  $\Pi/A$  curves, it is reasonable to ask if any corresponding differences in surface viscosity may be found. Variation in surface pressure as a function of molecular area must be the result, in the case of each compound, of a complex variation of stereoselective intramolecular interac-

(10) Furhop, J. H.; Fritsch, D. *Acc. Chem. Res.* **1986**, *19*, 130.

(11) Furhop, J. H.; David, H. H.; Mathieu, J.; Liman, U.; Winter, H. J.; Boekema, E. *J. Am. Chem. Soc.* **1986**, *108*, 1785.

(12) Jeffers, P. M.; Daen, J. *J. Phys. Chem.* **1965**, *69*, 2368.

(13) Morawetz, H.; Kandanem, A. Y. *J. Phys. Chem.* **1966**, *70*, 2995.

(14) Handa, T.; Nakagaki, M. *Colloid Polym. Sci.* **1979**, *257*, 374.

(15) Stewart, M.; Arnett, E. M. *Top. Stereochem.* **1982**, *13*.

(16) Defay, R. Doctoral Dissertation, Brussels, 1932.

(17) Crisp, D. J. *Surf. Chem. (Suppl. Res., London)* **1949**, *17*.

(18) Arnett, E. M.; Thompson, O. *J. Am. Chem. Soc.* **1981**, *103*, 968.

Table II. Rheological Properties of Diastereomeric Films at Various Surface Pressures II. (Free Energies of Activation for Viscous Flow,  $\Delta G_{\text{flow}}^{\ddagger}$ , Calculated from Surface Viscosities,  $\eta$ , eq 2)

$\Pi$ , dyn/cm	meso			dl		
	$\eta$ , surface mP	$\Delta G_{\text{flow}}^{\ddagger}$ , cal/mol		$\eta$ , surface mP	$\Delta G_{\text{flow}}^{\ddagger}$ , cal/mol	$\Delta \Delta G_{\text{flow}}^{\ddagger a}$ , cal/mol
			3,3'			
2.5	0.696 $\pm$ 0.065	16 033 $\pm$ 67		0.664 $\pm$ 0.028	16 241 $\pm$ 32	208 $\pm$ 74
5.0	0.832 $\pm$ 0.078	16 117 $\pm$ 67		0.840 $\pm$ 0.041	16 351 $\pm$ 36	243 $\pm$ 76
7.5	0.779 $\pm$ 0.026	16 068 $\pm$ 31		0.832 $\pm$ 0.034	16 322 $\pm$ 32	254 $\pm$ 45
10.0	0.801 $\pm$ 0.039	16 071 $\pm$ 41		0.792 $\pm$ 0.047	16 270 $\pm$ 43	199 $\pm$ 59
12.5	0.779 $\pm$ 0.030	16 040 $\pm$ 35		0.802 $\pm$ 0.047	16 259 $\pm$ 43	219 $\pm$ 55
15.0						
			6,6'			
2.5	0.689 $\pm$ 0.028	16 170 $\pm$ 33		0.702 $\pm$ 0.034	16 351 $\pm$ 35	181 $\pm$ 48
5.0	0.676 $\pm$ 0.019	16 132 $\pm$ 26		0.748 $\pm$ 0.027	16 314 $\pm$ 29	182 $\pm$ 39
7.5	0.697 $\pm$ 0.021	16 123 $\pm$ 27		0.875 $\pm$ 0.034	16 361 $\pm$ 31	238 $\pm$ 41
10.0	0.823 $\pm$ 0.014	16 192 $\pm$ 24		0.927 $\pm$ 0.031	16 328 $\pm$ 29	136 $\pm$ 38
12.5						
15.0						
			9,9'			
2.5	1.186 $\pm$ 0.134	16 423 $\pm$ 76		0.965 $\pm$ 0.061	16 784 $\pm$ 42	361 $\pm$ 87
5.0	1.061 $\pm$ 0.107	16 343 $\pm$ 70		0.922 $\pm$ 0.028	16 665 $\pm$ 23	322 $\pm$ 74
7.5	0.932 $\pm$ 0.075	16 246 $\pm$ 26		0.969 $\pm$ 0.020	16 648 $\pm$ 18	402 $\pm$ 32
10.0	0.849 $\pm$ 0.025	16 203 $\pm$ 28		1.002 $\pm$ 0.026	16 549 $\pm$ 22	346 $\pm$ 36
12.5	0.898 $\pm$ 0.026	16 198 $\pm$ 28		1.133 $\pm$ 0.096	16 552 $\pm$ 58	354 $\pm$ 64
15.0	0.906 $\pm$ 0.013	16 198 $\pm$ 19		1.176 $\pm$ 0.023	16 469 $\pm$ 20	271 $\pm$ 28
			12,12'			
2.5				1.074 $\pm$ 0.106	16 867 $\pm$ 62	
5.0				0.696 $\pm$ 0.027	16 525 $\pm$ 28	
7.5				0.857 $\pm$ 0.071	16 567 $\pm$ 54	
10.0				0.950 $\pm$ 0.043	16 532 $\pm$ 25	
12.5				1.094 $\pm$ 0.046	16 499 $\pm$ 33	
15.0				1.288 $\pm$ 0.047	16 477 $\pm$ 30	

<sup>a</sup> dl - meso.

tions, of the type described above, and of intermolecular interactions between the molecules as they lie in the surface and are gradually compressed. Rheological properties such as the surface viscosity might reasonably show considerable differences depending on the stereochemistry of the diacid and the surface pressure. Table II presents all of the surface shear viscosity data that we were able to measure for the eight diastereomeric diacids. Several trends may be perceived in the data. There is a general tendency (with exceptions) for viscosities to increase as a function of film pressure, as might be expected on the basis of greater intermolecular interactions. There are insignificant differences between meso and dl isomers for the 3,3'-compound and modest differences between meso and dl isomers for the 6,6'- and 9,9'-compounds. The largest differences are between the films cast from 6,6'- and 9,9'-isomers. Although the differences in surface shear viscosities between diastereomers are small for 6,6'- and 9,9'-diastereomers and negligible for 3,3'-diastereomers, the differences in free energies of activation to flow between diastereomers are significant and reflect directly the thermodynamic differences of these films at a constant surface pressure (Table II).

The free energies of activation to flow increase within a series of diastereomers (meso, dl) as the carbonyl group linkage is moved up the hydrocarbon chain. This may indicate increased intermolecular interactions as a result of lengthening the intramolecular head group to head group distance. For all diacid pairs, the dl diastereomer has a higher free energy of activation to flow than its meso isomer. On the basis of previous arguments, it is reasonable to relate this difference to the stereochemically dependent conformation at the air/water interface, which in some manner leads to different degrees of intermolecular entanglement.

Finally, it was found that the excess free energies of mixing<sup>19</sup> between the dl and meso diastereomers of the 6,6'- and 9,9'-surfactants showed significant differences that were dependent on the carbonyl position in each structural isomer.<sup>20</sup> These

differences in the stereochemically dependent intermolecular interactions are consistent with the observed variations in surface shear viscosity measurements.

### Conclusions

This study of four pairs of diastereomeric two-chain surfactants provides an unprecedented opportunity to compare the effects of stereochemistry on intramolecular interactions in monolayers. Force-area curves show a dramatic difference between behavior of each meso vs dl pair. All four of the meso isomers presented isotherms that are similar to each other and are strongly reminiscent of the behavior of ordinary long-chain fatty acids. In contrast, the isotherms for dl isomers are indicative of expanded monolayers starting at liftoff areas close to 200 Å<sup>2</sup>/molecule and ending in collapse plateaus at 25–30 dyn/cm. The different surface behavior of meso and dl isomers is interpreted readily in terms of the relative stereochemistry at the point of attachment of the two chains of the carbonyl bridge.

Precise determinations of surface viscosities were obtained with the modified Verger film balance. Although some differences were obtained in the viscosities as functions of surface pressure or stereochemistry, no significant interpretable trends can be reported. However, when the precise thermodynamic state of the film is considered at a constant, stable surface pressure/area relationship, then it is clear that there are differences in the free energies of activation for viscous flow not only between diastereomers (meso, dl) but also within a series of structural isomers (3,3'-12,12').

**Acknowledgment.** This work was supported by NIH Grants GM 28757 (to E.M.A.) and HL17921 (to N.A.P.) for which we are most appreciative. We are also glad to acknowledge the invaluable assistance of Majorie Richter. We acknowledge Dr. Dong Ok and Dr. Christopher Adams for the synthesis of the 6,6'- and 9,9'-diacids.

**Registry No.** dl-3,3', 114395-81-2; meso-3,3', 114395-80-1; dl-6,6', 114395-82-3; meso-6,6', 114422-54-7; dl-9,9', 114395-84-5; meso-9,9', 114395-83-4; dl-12,12', 114395-86-7; meso-12,12', 114395-85-6.

(19) Goodrich, F. C. *Proc. 2nd Inter. Congr. Surf. Act. 2nd 1957*, 1, 85.

(20) Harvey, N., unpublished results.